Letter

Scattering phase shifts from a quantum computer

Sanket Sharma [1] T. Papenbrock [1,2] and L. Platter[1,2]

[1]*Department of Physics and Astronomy, University of Tennessee, Knoxville, Tennessee 37996, USA*
[2]*Physics Division, Oak Ridge National Laboratory, Oak Ridge, Tennessee 37831, USA*

We calculate two-body scattering phase shifts on a quantum computer using a leading order short-range effective field theory Hamiltonian. The algorithm combines the variational quantum eigensolver and the quantum subspace expansion. As an example, we consider scattering in the deuteron $^3S_1$ partial wave. We calculate scattering phase shifts with a quantum simulator and on real hardware. We also study how noise impacts these calculations and discuss noise mitigation required to extend our work to larger quantum processing units. With current hardware, up to five superconducting qubits can produce acceptable results, and larger calculations will require a significant noise reduction.

Introduction. Decades ago, Feynman [1] proposed quantum computers as the ultimate tool to simulate quantum mechanical systems and thought their development was a worthwhile and interesting task in itself. The recent progress in quantum hardware regarding fidelities and qubit count [2] and in quantum algorithms has intrigued researchers across all fields of physics [3–5]. In a few years, the number of qubits used in simulations has grown from a few [6] to 100 [7]. Nuclear physicists have embraced the potential of this new technology and explored simple models [8–15], studied entanglement [16–18], modeled neutrino physics [19–22], and proposed algorithms for state preparations [23–27]. However, the critical analysis by Lee *et al.* [28] suggests that classical computations of molecular structure in quantum chemistry might be harder to beat on quantum computers than originally thought because there are powerful classical algorithms that permit accurate computations at a cost that increases polynomially (and not exponentially) with increasing system size. In contrast, the simulation of dynamical processes in real-time still poses formidable challenges in classical computing, and many efforts are dedicated to exploring those in quantum computing [29–31].

Of course, many time-dependent phenomena can be computed more efficiently in the energy domain, e.g., via the scattering matrix or response functions [19,32–34]. In elastic scattering, the phase shifts determine the scattering matrix, and—strictly speaking—their computation at arbitrary energies requires the solution of a continuum problem. However, phase shifts at discrete energies can be computed within a bound-state approach based on finite Hilbert spaces [35]. Nuclear *ab initio* calculations of scattering phase shifts are challenging [36–39]. They are also challenging for simple models on noisy hardware because energies of excited states need to be computed accurately. In this Letter, we show how to meet this challenge.

One important algorithm is the variational quantum eigensolver (VQE) [40,41]. It returns the minimum energy for a variational ansatz provided. VQE is a hybrid algorithm that pairs an optimizer running on a classical computer with the evaluation of energy expectation values on a quantum device. For many applications in physics and chemistry, VQE has been a popular choice since it facilitates the calculation of the ground state of a Hamiltonian if a good trial wave function is given, see Refs. [6,8,42,43] for early examples and Ref. [44] for a review.

Recently, a similar hybrid approach, known as the quantum subspace expansion, was proposed to calculate the excited state spectrum of a quantum mechanical system [45]. In this approach, one computes the Hamiltonian matrix elements on the quantum hardware by using excitation operators that act on the ground state obtained from VQE. The resulting matrix is then diagonalized on a classical computer. This approach has been used to compute the spectra of the hydrogen molecule [46], to simulate spin defects [47], and for the simulation of periodic materials [48].

Here, we extract scattering phase shifts using a quantum computer. Our approach combines the VQE algorithm, finite volume methods [35] developed for the harmonic oscillator basis [38,49,50], and the quantum subspace expansion. At the heart of this method lies that the quantum subspace expansion yields low-lying, positive-energy eigenvalues of the Hamiltonian. In finite volume problems, these can be related to scattering observables such as phase shifts. We start by discussing the two-nucleon Hamiltonian and the relation between finite volume eigenvalues and phase shifts. We then present our results obtained on real hardware and simulators and discuss how noise impacts the calculations on larger quantum processing units (QPUs). Finally, we end with a brief summary and outlook.

Two-nucleon Hamiltonian. Throughout this work we focus entirely on the $^3S_1$ partial wave of the nucleon-nucleon system. This fixes the spin/isospin degrees of freedom and we can limit the discussion to S waves in the center-of-mass system. Thus, we deal with a one-body potential-scattering

problem. We employ a Hamiltonian from short-range effective field theory (EFT) [51,52] that was also used in Refs. [8,53]. This EFT is a systematic low-energy expansion in powers of R/a, where R denotes the range of the interaction and a the two-body scattering length. This approach has been used successfully to calculate a number of few-nucleon observables to high accuracy [54]. Here, we will use only the leading order of this approach that also maps directly onto the zero-range limit. One possible way to implement this EFT is to use a separable interaction

$$V = V_0 |g\rangle\langle g|, \tag{1}$$

where V_0 is the coupling constant adjusted to reproduce one two-body observable for an ultraviolet cutoff Λ that is encoded in the form factor $|g\rangle$, which we specify below. The two-body problem can be solved exactly for a separable interaction, and the S-wave two-body on-shell t matrix becomes [55]

$$t(p) = \frac{4\pi}{m} \frac{\langle p|g\rangle\langle g|p\rangle}{1/V_0 - \langle g|G_0|g\rangle}, \tag{2}$$

where $G_0(E)|q\rangle = [E - \frac{q^2}{m} + i\epsilon]^{-1}|q\rangle$ denotes the free two-body Green's function for identical particles with mass m. In the finite harmonic oscillator basis with N states, the Hamiltonian in the center-of-mass system of the $^3S_1$ partial wave is written as

$$H_N = \sum_{n,n'=0}^{N-1} \langle n'|(T+V)|n\rangle a_{n'}^\dagger a_n. \tag{3}$$

Here, operators $a^\dagger$ (a_n) create (annihilate) a two-nucleon state in the nth harmonic oscillator S-wave state. The kinetic energy and the separable potential are

$$\langle n'|T|n\rangle = \frac{\hbar\omega}{2}\left[\left(2n + \tfrac{3}{2}\right)\delta_n^{n'} + \sqrt{n\left(n+\tfrac{1}{2}\right)}\delta_n^{n'+1} \right.$$
$$\left. - \sqrt{(n+1)\left(n+\tfrac{3}{2}\right)}\delta_n^{n'-1} \right],$$
$$\langle n'|V|n\rangle = V_0 \delta_n^0 \delta_n^{n'}, \tag{4}$$

where the coupling of the $V_0 = -5.68658111$ MeV is adjusted to reproduce the deuteron binding energy in the limit of an infinite number of harmonic oscillator states and $\hbar\omega = 7$ MeV. The Kronecker δ functions reflect that we use the lowest harmonic oscillator orbital for the form factor $|g\rangle$, i.e., $\langle q|g\rangle = b^{1/2}\pi^{-1/4}\exp\left(-q^2 b^2/2\right)$, where b is the oscillator length.

Though we are dealing technically with a one-body system, the second-quantized form of the Hamiltonian (3) is attractive for quantum computing. The operators $a_n^\dagger$ and a_n become spin-lowering and spin-rising operators, respectively, when acting on qubits, and the mapping uses the Jordan-Wigner transform [8]. Within this work, an unoccupied and occupied state $|n\rangle$ of the harmonic oscillator will correspond to the state $|0\rangle$ and $|1\rangle$, respectively, of qubit n. We use the VQE algorithm to find the ground state of the system. This requires an ansatz with parameters that can be optimized to find the lowest possible energy. We use the unitary coupled cluster (UCC) ansatz also

used in Refs. [8,53]. The ansatz circuit we implemented is similar to the one in [53].

The quantum subspace expansion. The quantum subspace expansion was developed by McClean *et al.* [45] to calculate excited states. Like VQE, it is a hybrid algorithm that relies on a combination of classical and quantum computing. First, the VQE algorithm is used to generate the ground-state wave function of the Hamiltonian under consideration. This ground-state wave function $|\Psi\rangle$ is used in combination with excitation operators to generate a subspace in which the Hamiltonian can be diagonalized with a classical computer. Here, we will use single-particle excitation operators

$$e_\alpha = a_j^\dagger a_l, \tag{5}$$

where $j, l = 0, \ldots, N-1$ and α is a single label that uniquely identifies j and l (e.g., $\alpha = Nj + l$). We note that this approach identifies all excitations in the Hilbert space. This completeness of the basis is not achievable in many practical applications due to the enormous size of Hilbert spaces. Instead, one could identify a subset of relevant excitations and then diagonalize the Hamiltonian in that basis. This is essentially the generator coordinate method [56].

On the quantum computer, we evaluate the matrix elements

$$\tilde{H}_{\alpha\beta} = \langle\Psi|e_\alpha^\dagger H e_\beta|\Psi\rangle, \tag{6}$$

and the overlap matrix elements

$$\tilde{S}_{\alpha\beta} = \langle\Psi|e_\alpha^\dagger e_\beta|\Psi\rangle. \tag{7}$$

Now, we solve the generalized eigenvalue problem

$$\tilde{H}|\Psi\rangle = E\tilde{S}|\Psi\rangle \tag{8}$$

on a classical computer and employ the usual techniques, see, e.g., Ref. [56].

This overlap matrix has only N nonzero eigenvalues, and we discard the eigenvectors corresponding to zero eigenvalues. In the presence of noise, we keep the N eigenvectors with the largest eigenvalues. The resulting energy eigenvalues are E_i, and the corresponding momenta are denoted as $k_i = \sqrt{2\mu E_i}$. All our results from quantum subspace expansion were obtained as described above. However, this $N^2 \times N^2$ problem can be reduced to an $N \times N$ problem by setting l to 0 in Eq. (5) and solving the resulting smaller generalized eigenvalue problem. We have verified on the simulator for the five- and seven-qubit systems that this approach leads to the same results within statistical fluctuations.

Having obtained the ground state wave function $|\Psi\rangle$ on the quantum device, we then obtain the phase shifts from the positive energy eigenvalues of the Hamiltonian. For this, we follow the approach described in Ref. [50]. The key insight is briefly described as follows: Employing a finite harmonic oscillator basis transforms the scattering continuum into a discrete set of states confined within a finite volume. This effectively imposes Dirichlet boundary conditions at a specific radial distance $r = L$. The hard wall radius L depends on N, $\hbar\omega$, and the scattering energy. To compute L, one must first diagonalize the kinetic energy operator $\hat{T}$ in the finite harmonic oscillator basis. This yields a spectrum of energies T_i and corresponding momenta $p_i = \sqrt{2\mu T_i}$. In position space, the corresponding eigenfunctions resemble those of
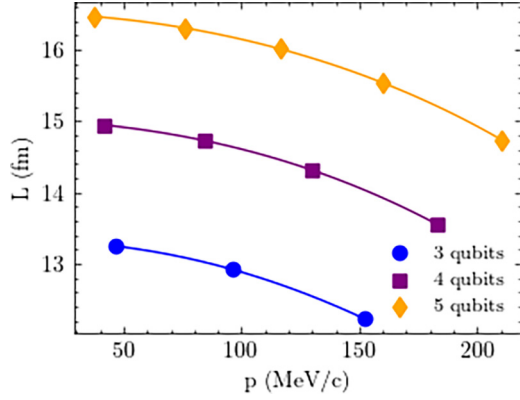
FIG. 1. Box size L as a function of the relative momentum p for the simulations of systems with three, four, and five qubits. The markers are at the relative momenta of the eigenvalues of the kinetic energy. The solid lines are interpolation curves.

FIG. 2. Scattering phase shifts δ as a function of the relative momentum k. The solid line denotes the analytical results. The circles, squares, and diamonds give the results obtained with a three-, four-, and five-qubit simulation, respectively. Simulation results were obtained on the *ibmq_jakarta* QPU.

a spherical cavity with a radius L. The location of the ith zero of the spherical S-wave Bessel function $j_0(p_i L_i \hbar)$ then determines $L = L(p_i) \equiv L_i$. From the resulting set of p_i and L_i we can then generate a smooth and continuous interpolation function $L(p)$. Figure 1 shows box sizes $L(p)$ as a function of the relative momentum p for three-, four-, and five-qubit systems. Given that the kinetic energy operator $\hat{T}$ is diagonalized classically, the calculation of $L(p)$ in unaffected by quantum noise. The observed convexity and small curvature of the resulting curves suggest that these interpolations are very reliable, leaving therefore very little room for additional uncertainties due to this approach of determining the effective box size $L(\hbar k_i)$.

The phase shift for the ith momentum k_i is then given by

$$\tan \delta_0(k_i) = \frac{j_0(k_i L(\hbar k_i))}{\eta_0(k_i L(\hbar k_i))}, \tag{9}$$

where j_0 and η_0 denote the S-wave spherical Bessel and Neumann functions, respectively. The above equation reflects that the radial wave function has to be zero at L as required by the hard wall boundary condition. When L is known, Eq. (9) yields a result that matches exactly with the analytical result.

Results. Our quantum computations used IBMQ machines. Throughout this work, we employed noise mitigation of readout errors. We measured the complete assignment matrix to perform readout error mitigation on the noisy counts received from the QPU. For this, we include circuits in which we initialize the qubits to combinations of zeros and ones. We then multiply the inverse of this assignment matrix with the counts to obtain the noise-mitigated counts. For three qubits, the ground state depends on two parameters, and we compute energy expectation values on the quantum hardware using a two-dimensional grid. In our calculations involving more than three qubits, we assume that the deuteron ground state was previously determined by techniques such as VQE and instead use the ground state from an exact diagonalization. We pass the exact ground state to our code and then evaluate the
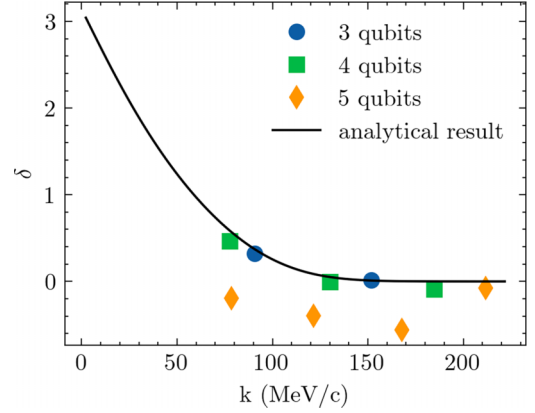
matrix elements required for the quantum subspace expansion on quantum hardware. The computations on N qubits yield $N-1$ excited states, and we determine the corresponding phase shifts using Eq. (9).

In Fig. 2, we show results for three, four, and five qubits on the *ibmq_jakarta* QPU as circles, squares, and diamonds, respectively. The solid line shows the results obtained from the analytical expression given in Eq. (2). Our results for the three qubits agree with the analytical result. This is encouraging as the corresponding bound state calculation requires error mitigation to obtain accurate results [8]. As we increase the number of qubits, the agreement worsens, and the five qubit results are inaccurate.

Our method produces phase shifts at momenta determined by the harmonic oscillator frequency. The effective field theory allows us to vary the harmonic oscillator frequency (while adjusting the potential strength V_0 such that the deuteron bound state energy is reproduced correctly in the infinite oscillator basis). This permits us to compute phase shifts at different momenta at a fixed number of qubits N.

We generated five additional interactions and now consider oscillator frequencies $\hbar\omega = 5, 6, 7, 8, 9, 10$ MeV. The corresponding momentum cutoffs are $\Lambda = 128, 140, 152, 162, 172, 181$ MeV, respectively. For each frequency, we repeat the calculations of phase shifts and show the corresponding results, obtained on three qubits, in Fig. 3. The analytical results for our six interactions vary slightly due to remaining regulator dependence in the renormalization process: All interactions essentially reproduce the scattering length (i.e., they agree on the slope of the phase shifts at zero momentum) but differ in the effective range. We see that the analytical results differ, as expected, at larger momenta and that the phase shifts vanish at momenta above the respective cutoff. In all cases, the results from quantum computing agree with the corresponding analytical data.

Figure 4 shows the results obtained on four qubits, using the QPU *ibm_nairobi*. Here, the low-energy phase shifts are
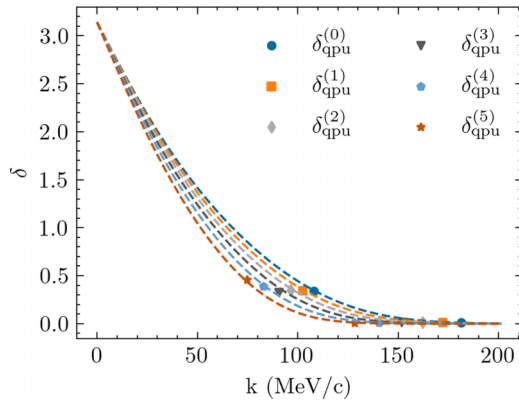
FIG. 3. The data points are the phase shifts obtained using six different interactions (with the oscillator frequency and the momentum cutoff increasing from left to right) using three qubits. The dashed lines are the analytical results corresponding to the interaction represented by the same color. The circles denote the results obtained with the QPU *ibmq_jakarta*.

accurate. At higher energies, the phase shifts are still close to the analytical results, but they essentially vanish. This suggests that it will be challenging to employ more qubits in the computations using quantum hardware.

We computed the total χ^2 deviation between the phase shifts from simulations and analytical results based on a model space of N qubits. The simulations employ the *ibmq_guadalupe* noise model. The results, shown in Fig. 5, suggest that there is a transition at about $N \approx 5$ beyond which quantum computations become too limited by noise.

To understand this apparent limitation, we studied the impact of noise on larger systems using a QPU simulator using again the *ibmq_guadalupe* noise model. We are interested in quantifying how much noise is tolerable to compute accurate phase shifts on a fixed number of qubits. To address this point, we modified Qiskit's noise model source code. We introduced a single scaling factor $\eta \leqslant 1$ that simultaneously reduces the one-qubit gate errors, two-qubit gate errors, and the readout
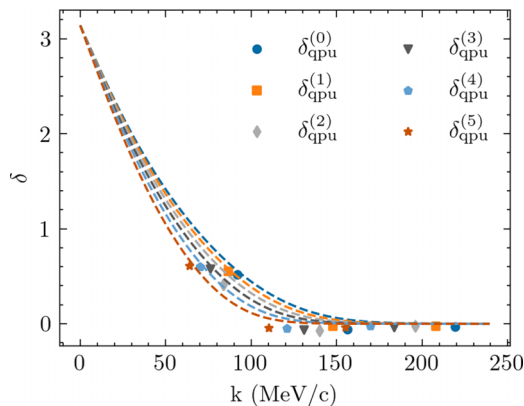

FIG. 4. Phase shifts obtained using six different interactions using four qubits. The dashed lines denote the analytical results corresponding to the interaction represented by the same color. The circles denote the results obtained with the QPU *ibm_nairobi*.
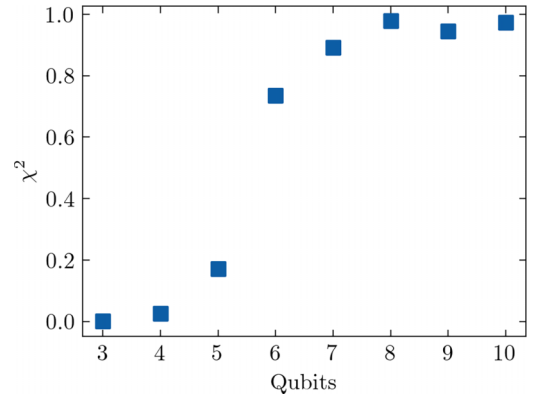

FIG. 5. χ^2 as a function of number of qubits.

error. For a given system size N we decreased η using the *ibmq_guadalupe* noise model until an approximate agreement between simulation and analytical results was achieved. The estimated value of η obtained in this way is plotted against the number of qubits in Fig. 6. We see that there is a jump as one goes from four to five qubits, and an order-of-magnitude in noise reduction is required for computations on more than six qubits.

Summary. We computed nucleon-nucleon scattering phase shifts on a quantum device by combining hybrid quantum algorithms with finite-volume approaches to scattering. We employed the quantum subspace expansion to compute discrete continuum states and mapped those to scattering phase shifts. While current superconducting hardware allows one only to treat simple models, *ab initio* computations of scattering phase shifts are expensive [36–39]. It is here that error-corrected quantum computing could be advantageous in the future.

Using noise mitigation to correct readout errors only allowed us to perform accurate computations with up to four or five superconducting qubits. Our study of this problem revealed that an order-of-magnitude reduction in readout errors and one- and two-qubit gate errors is necessary for accurate quantum computations with significantly more qubits. We believe that this result will also hold for other applications
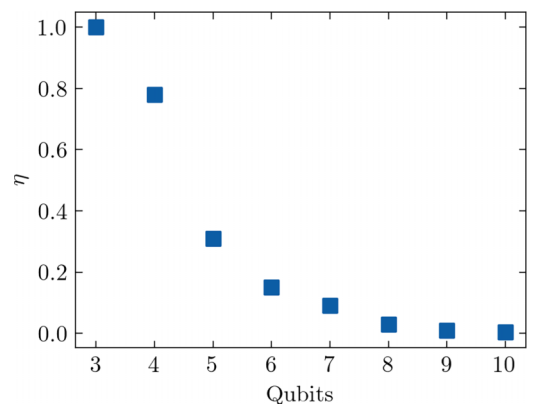

FIG. 6. Estimated noise scaling factor η required to produce acceptable results as a function of the number of qubits.

[1] R. P. Feynman, Simulating physics with computers, Int. J. Theor. Phys. **21**, 467 (1982).

[2] G. T. Byrd and Y. Ding, Quantum computing: Progress and innovation, Computer **56**, 20 (2023).

[3] Y. Cao, J. Romero, J. P. Olson, M. Degroote, P. D. Johnson, M. Kieferová, I. D. Kivlichan, T. Menke, B. Peropadre, N. P. D. Sawaya, S. Sim, L. Veis, and A. Aspuru-Guzik, Quantum chemistry in the age of quantum computing, Chem. Rev. **119**, 10856 (2019).

[4] N. Klco, A. Roggero, and M. J. Savage, Standard model physics and the digital quantum revolution: thoughts about the interface, Rep. Prog. Phys. **85**, 064301 (2022).

[5] T. Ayral, P. Besserve, D. Lacroix, and E. A. Ruiz Guzman, Quantum computing with and for many-body physics, Eur. Phys. J. A **59**, 227 (2023).

[6] A. Kandala, A. Mezzacapo, K. Temme, M. Takita, M. Brink, J. M. Chow, and J. M. Gambetta, Hardware-efficient variational quantum eigensolver for small molecules and quantum magnets, Nature (London) **549**, 242 (2017).

[7] R. C. Farrell, M. Illa, A. N. Ciavarella, and M. J. Savage, Scalable circuits for preparing ground states on digital quantum computers: The Schwinger model vacuum on 100 qubits, PRX Quantum **5**, 020315 (2024).

[8] E. F. Dumitrescu, A. J. McCaskey, G. Hagen, G. R. Jansen, T. D. Morris, T. Papenbrock, R. C. Pooser, D. J. Dean, and P. Lougovski, Cloud quantum computing of an atomic nucleus, Phys. Rev. Lett. **120**, 210501 (2018).

[9] N. Klco, E. F. Dumitrescu, A. J. McCaskey, T. D. Morris, R. C. Pooser, M. Sanz, E. Solano, P. Lougovski, and M. J. Savage, Quantum-classical computations of Schwinger model dynamics using quantum computers, Phys. Rev. A **98**, 032331 (2018).

[10] M. J. Cervia, A. B. Balantekin, S. N. Coppersmith, C. W. Johnson, P. J. Love, C. Poole, K. Robbins, and M. Saffman, Lipkin model on a quantum computer, Phys. Rev. C **104**, 024305 (2021).

[11] W. Du, J. P. Vary, X. Zhao, and W. Zuo, Quantum simulation of nuclear inelastic scattering, Phys. Rev. A **104**, 012611 (2021).

[12] I. Stetcu, A. Baroni, and J. Carlson, Variational approaches to constructing the many-body nuclear ground state for quantum computing, Phys. Rev. C **105**, 064308 (2022).

[13] O. Kiss, M. Grossi, P. Lougovski, F. Sanchez, S. Vallecorsa, and T. Papenbrock, Quantum computing of the ^{6}Li nucleus via ordered unitary coupled clusters, Phys. Rev. C **106**, 034325 (2022).

[14] M. Q. Hlatshwayo, Y. Zhang, H. Wibowo, R. LaRose, D. Lacroix, and E. Litvinova, Simulating excited states of the Lipkin model on a quantum computer, Phys. Rev. C **106**, 024319 (2022).

[15] A. Pérez-Obiol, A. M. Romero, J. Menéndez, A. Rios, A. García-Sáez, and B. Juliá-Díaz, Nuclear shell-model simulation in digital quantum computers, Sci. Rep. **13**, 12291 (2023).

[16] S. R. Beane, D. B. Kaplan, N. Klco, and M. J. Savage, Entanglement suppression and emergent symmetries of strong interactions, Phys. Rev. Lett. **122**, 102001 (2019).

[17] C. Robin, M. J. Savage, and N. Pillet, Entanglement rearrangement in self-consistent nuclear structure calculations, Phys. Rev. C **103**, 034325 (2021).

[18] C. Gu, Z. H. Sun, G. Hagen, and T. Papenbrock, Entanglement entropy of nuclear systems, Phys. Rev. C **108**, 054309 (2023).

[19] A. Roggero, A. C. Y. Li, J. Carlson, R. Gupta, and G. N. Perdue, Quantum computing for neutrino-nucleus scattering, Phys. Rev. D **101**, 074038 (2020).

[20] M. J. Cervia, P. Siwach, A. V. Patwardhan, A. B. Balantekin, S. N. Coppersmith, and C. W. Johnson, Collective neutrino oscillations with tensor networks using a time-dependent variational principle, Phys. Rev. D **105**, 123025 (2022).

[21] V. Amitrano, A. Roggero, P. Luchi, F. Turro, L. Vespucci, and F. Pederiva, Trapped-ion quantum simulation of collective neutrino oscillations, Phys. Rev. D **107**, 023007 (2023).

[22] M. Illa and M. J. Savage, Multi-neutrino entanglement and correlations in dense neutrino systems, Phys. Rev. Lett. **130**, 221003 (2023).

[23] D. Lacroix, Symmetry-assisted preparation of entangled many-body states on a quantum computer, Phys. Rev. Lett. **125**, 230502 (2020).

[24] A. Roggero, C. Gu, A. Baroni, and T. Papenbrock, Preparation of excited states for nuclear dynamics on a quantum computer, Phys. Rev. C **102**, 064624 (2020).

[25] K. Choi, D. Lee, J. Bonitati, Z. Qian, and J. Watkins, Rodeo algorithm for quantum computing, Phys. Rev. Lett. **127**, 040505 (2021).

[26] P. F. Bedaque, R. Khadka, G. Rupak, and M. Yusf, Radiative processes on a quantum computer, arXiv:2209.09962.

[27] E. A. Coello Pérez, J. Bonitati, D. Lee, S. Quaglioni, and K. A. Wendt, Quantum state preparation by adiabatic evolution with custom gates, Phys. Rev. A **105**, 032403 (2022).

[28] S. Lee, J. Lee, H. Zhai, Y. Tong, A. M. Dalzell, A. Kumar, P. Helms, J. Gray, Z.-H. Cui, W. Liu, M. Kastoryano, R. Babbush, J. Preskill, D. R. Reichman, E. T. Campbell, E. F. Valeev, L. Lin, and G. K.-L. Chan, Evaluating the evidence for exponential quantum advantage in ground-state quantum chemistry, Nat. Commun. **14**, 1952 (2023).

[29] E. A. Martinez, C. A. Muschik, P. Schindler, D. Nigg, A. Erhard, M. Heyl, P. Hauke, M. Dalmonte, T. Monz, P. Zoller, and R. Blatt, Real-time dynamics of lattice gauge theories with a few-qubit quantum computer, Nature (London) **534**, 516 (2016).

[30] S. Barison, F. Vicentini, and G. Carleo, An efficient quantum algorithm for the time evolution of parameterized circuits, Quantum **5**, 512 (2021).

[31] K. Klymko, C. Mejuto-Zaera, S. J. Cotton, F. Wudarski, M. Urbanek, D. Hait, M. Head-Gordon, K. B. Whaley, J. Moussa, N. Wiebe, W. A. de Jong, and N. M. Tubman, Real-time evolution for ultracompact Hamiltonian eigenstates on quantum hardware, PRX Quantum **3**, 020323 (2022).

[32] V. D. Efros, W. Leidemann, G. Orlandini, and N. Barnea, The Lorentz integral transform (LIT) method and its applications to perturbation-induced reactions, J. Phys. G: Nucl. Part. Phys. **34**, R459 (2007).

[33] S. Bacca and S. Pastore, Electromagnetic reactions on light nuclei, J. Phys. G: Nucl. Part. Phys. **41**, 123002 (2014).

[34] A. Roggero and J. Carlson, Linear response on a quantum computer, Phys. Rev. C **100**, 034610 (2019).

[35] E. J. Heller and H. A. Yamani, New L^2 approach to quantum scattering: Theory, Phys. Rev. A **9**, 1201 (1974).

[36] K. M. Nollett, S. C. Pieper, R. B. Wiringa, J. Carlson, and G. M. Hale, Quantum Monte Carlo calculations of neutron-α scattering, Phys. Rev. Lett. **99**, 022502 (2007).

[37] S. Quaglioni and P. Navrátil, *Ab initio* many-body calculations of $n-^3$H, $n-^4$He, $p-^{3,4}$He, and $n-^{10}$Be scattering, Phys. Rev. Lett. **101**, 092501 (2008).

[38] A. M. Shirokov, A. I. Mazur, J. P. Vary, and E. A. Mazur, Inverse scattering J-matrix approach to nucleon-nucleus scattering and the shell model, Phys. Rev. C **79**, 014610 (2009).

[39] S. Elhatisari, D. Lee, G. Rupak, E. Epelbaum, H. Krebs, T. A. Lähde, T. Luu, and U.-G. Meißner, *Ab initio* alpha–alpha scattering, Nature (London) **528**, 111 (2015).

[40] A. Peruzzo, J. McClean, P. Shadbolt, M.-H. Yung, X.-Q. Zhou, P. J. Love, A. Aspuru-Guzik, and J. L. O'Brien, A variational eigenvalue solver on a photonic quantum processor, Nat. Commun. **5**, 4213 (2014).

[41] J. R. McClean, J. Romero, R. Babbush, and A. Aspuru-Guzik, The theory of variational hybrid quantum-classical algorithms, New J. Phys. **18**, 023023 (2016).

[42] P. J. J. O'Malley, R. Babbush, I. D. Kivlichan, J. Romero, J. R. McClean, R. Barends, J. Kelly, P. Roushan, A. Tranter, N. Ding, B. Campbell, Y. Chen, Z. Chen, B. Chiaro, A. Dunsworth, A. G. Fowler, E. Jeffrey, E. Lucero, A. Megrant, J. Y. Mutus *et al.*,

Scalable quantum simulation of molecular energies, Phys. Rev. X **6**, 031007 (2016).

[43] Y. Shen, X. Zhang, S. Zhang, J.-N. Zhang, M.-H. Yung, and K. Kim, Quantum implementation of the unitary coupled cluster for simulating molecular electronic structure, Phys. Rev. A **95**, 020501(R) (2017).

[44] J. Tilly, H. Chen, S. Cao, D. Picozzi, K. Setia, Y. Li, E. Grant, L. Wossnig, I. Rungger, G. H. Booth, and J. Tennyson, The variational quantum eigensolver: A review of methods and best practices, Phys. Rep. **986**, 1 (2022).

[45] J. R. McClean, M. E. Kimchi-Schwartz, J. Carter, and W. A. de Jong, Hybrid quantum-classical hierarchy for mitigation of decoherence and determination of excited states, Phys. Rev. A **95**, 042308 (2017).

[46] J. I. Colless, V. V. Ramasesh, D. Dahlen, M. S. Blok, M. E. Kimchi-Schwartz, J. R. McClean, J. Carter, W. A. de Jong, and I. Siddiqi, Computation of molecular spectra on a quantum processor with an error-resilient algorithm, Phys. Rev. X **8**, 011021 (2018).

[47] B. Huang, M. Govoni, and G. Galli, Simulating the electronic structure of spin defects on quantum computers, PRX Quantum **3**, 010339 (2022).

[48] N. Yoshioka, T. Sato, Y. O. Nakagawa, Y.-Y. Ohnishi, and W. Mizukami, Variational quantum simulation for periodic materials, Phys. Rev. Res. **4**, 013052 (2022).

[49] T. Luu, M. J. Savage, A. Schwenk, and J. P. Vary, Nucleon-nucleon scattering in a harmonic potential, Phys. Rev. C **82**, 034003 (2010).

[50] S. N. More, A. Ekström, R. J. Furnstahl, G. Hagen, and T. Papenbrock, Universal properties of infrared oscillator basis extrapolations, Phys. Rev. C **87**, 044326 (2013).

[51] D. B. Kaplan, M. J. Savage, and M. B. Wise, A new expansion for nucleon-nucleon interactions, Phys. Lett. B **424**, 390 (1998).

[52] D. B. Kaplan, M. J. Savage, and M. B. Wise, Two nucleon systems from effective field theory, Nucl. Phys. B **534**, 329 (1998).

[53] O. Shehab, K. Landsman, Y. Nam, D. Zhu, N. M. Linke, M. Keesan, R. C. Pooser, and C. Monroe, Toward convergence of effective-field-theory simulations on digital quantum computers, Phys. Rev. A **100**, 062319 (2019).

[54] H. W. Hammer, S. König, and U. van Kolck, Nuclear effective field theory: status and perspectives, Rev. Mod. Phys. **92**, 025004 (2020).

[55] J. R. Taylor, *Scattering Theory: The Quantum Theory of Nonrelativistic Collisions* (John Wiley & Sons, Inc., New York, 1972).

[56] P. Ring and P. Schuck, *The Nuclear Many-Body Problem* (Springer, Heidelberg, 1980).